Global Nuclear Fuel

A Joint Venture of GE, Toshiba, & Hitachi

NEDO-33241
eDRFSection 0000-0047-8945
November 2005

Licensing Topical Report

GE14 Fuel Rod Thermal-Mechanical Design Report

S. B. Shelton
R. A. Rand

NON PROPRIETARY NOTICE

This is a non proprietary version of the document NEDE-33241P, which has the proprietary information removed. Portions of the document that have been removed are indicated by an open and closed bracket as shown here [[ ]].

IMPORTANT NOTICE REGARDING CONTENTS OF THIS REPORT

Please Read Carefully

The information contained in this document is furnished as reference material for GE14 fuel rod thermal-mechanical design. The only undertakings of Global Nuclear Fuel (GNF) with respect to information in this document are contained in the contracts between GNF and the participating utilities in effect at the time this report is issued, and nothing contained in this document shall be construed as changing those contracts. The use of this information by anyone other than that for which it is intended is not authorized; and with respect to any unauthorized use, GNF makes no representation or warranty, and assumes no liability as to the completeness, accuracy, or usefulness of the information contained in this document.

CONTENTS

FIGURES IV

TABLES V

ABSTRACT VI

ACRONYMS AND ABBREVIATIONS VII

1. INTRODUCTION 1

2. FUEL ROD DESCRIPTION 3

3. DESIGN CRITERIA 9

3.1 Cladding Lift-Off / Fuel Rod Internal Pressure (Item 1 of Table 3-1) 9
3.2 Fuel Temperature (Melting, Item 2 of Table 3-1) 9
3.3 Cladding Strain 10
3.3.1 High Strain Rate (Anticipated Operational Occurrences, Item 3 of Table 3-1) 10
3.3.2 Low Strain Rate (Steady-State Operation, no limit in Table 3-1) 10
3.4 Dynamic Loads / Cladding Fatigue (Item 4 of Table 3-1) 11
3.5 Elastic Buckling / Cladding Creep Collapse (Item 5 of Table 3-1) 11
3.6 Fuel Rod Stresses (Item 6 of Table 3-1) 12
3.7 Fuel Rod Hydrogen (Item 7 of Table 3-1) 12

4. DESIGN ANALYSES DESCRIPTION 14

4.1 Worst Tolerance Analyses 16
4.2 Statistical Analyses 18
4.2.1 Fuel Rod Internal Pressure 20
4.2.2 Fuel Pellet Temperature 20
4.2.3 Cladding Fatigue Analysis 20
4.3 Cladding Creep Collapse 22
4.4 Fuel Rod Stress Analysis 22
4.5 Thermal and Mechanical Overpowers 22

5. DESIGN ANALYSIS RESULTS 24

5.1 Cladding Lift-Off / Fuel Rod Internal Pressure 24

5.2 Thermal and Mechanical Overpowers **24**
5.2.1 Fuel Temperture 24
5.2.2 Cladding Strain 24
5.3 Cladding Corrosion **25**
5.4 Cladding Hydrogen Content **25**
5.5 Cladding Creep Collapse **26**
5.6 Fuel Rod Stresses/Strains **26**
5.7 Dynamic Loads / Cladding Fatigue **26**

6. FUEL OPERATING EXPERIENCE UPDATE **28**

REFERENCES **30**

APPENDIX A STATISTICAL DISTRIBUTION PARAMETERS **A-1**

APPENDIX B FUEL ROD PROCESSING **B-1**

FIGURES

FIGURE 2-1 FUEL ROD 7
FIGURE 2-2 FUEL PELLET SKETCH 8
FIGURE 4-1 DESIGN BASIS POWER VERSUS EXPOSURE ENVELOPE (TYPICAL) 15
FIGURE 4-2 AXIAL POWER DISTRIBUTIONS (FULL LENGTH FUEL ROD) 16
FIGURE 4-3 THERMAL AND MECHANICAL OVERPOWERS (SCHEMATIC) 23
FIGURE A-1 UO_2 PELLET DENSITY STATISTICAL SPECIFICATION AND SAMPLING RESULTS A-2
FIGURE A-2 GSTRM FUEL TEMPERATURE EXPERIMENTAL QUALIFICATION A-3
FIGURE A-3 GSTRM FISSION GAS RELEASE EXPERIMENTAL QUALIFICATION A-5
FIGURE A-4 EFFECT OF +2 SIGMA BIAS IN MODEL PREDICTION UNCERTAINTY ON FISSION GAS RELEASE PREDICTIONS A-6
FIGURE A-5 CLADDING CORROSION MODEL STATISTICAL PARAMETERS A-7

TABLES

TABLE 2-1 FUEL PELLET CHARACTERISTICS 4
TABLE 2-2 FUEL ROD CHARACTERISTICS 5
TABLE 2-3 CLADDING TUBE CHARACTERISTICS 6
TABLE 3-1 FUEL ROD THERMAL-MECHANICAL DESIGN CRITERIA 13
TABLE 4-1 WORST TOLERANCE ANALYSIS MANUFACTURING PARAMETER BIASES 17
TABLE 4-2 GSTRM PARAMETERS VARIED STATISTICALLY 18
TABLE 4-3 FATIGUE ANALYSIS POWER CYCLES 21
TABLE 5-1 FUEL ROD INTERNAL PRESSURE AND DESIGN RATIO 24
TABLE 5-2 LFWH, INADVERTENT HPCS, HPCI, RCIC INJECTION, RWE-OUTSIDE ERROR CELL OVERPOWER LIMITS 25
TABLE 5-3 RESULTS OF CLADDING STRESS ANALYSIS 26
TABLE 5-4 CLADDING-FATIGUE USAGE 27
TABLE 6-1 GE11/13 (9X9) EXPERIENCE SUMMARY AS OF 10/31/05 28
TABLE 6-2 GE12/14 (10X10) EXPERIENCE SUMMARY AS OF 10/31/05 29
TABLE B-1 TUBE SHELL ALLOY COMPOSITION AND OXYGEN CONCENTRATION B-1
TABLE B-2 FINISHED TUBE CHEMISTRY - ZIRCALOY-2 PORTION B-2
TABLE B-3 FINISHED TUBE CRYSTALLOGRAPHIC TEXTURE - ZIRCALOY-2 PORTION B-2

ABSTRACT

In this report, the design analyses of UO_2 and $(U,Gd)O_2$ fuel rods for the GE14 fuel assembly are summarized for use in BWR/3-6 and ABWR power stations. The analyses results demonstrate that all design criteria applicable to the fuel rod thermal-mechanical design are satisfied for operation of the GE14 fuel design out to peak pellet exposures of [[ ]] and a maximum operating time of [[ ]]. The specific design criteria which are addressed by this report include:

1) Fuel rod internal pressure
2) Fuel melting
3) Pellet-cladding mechanical interaction (PCMI)
4) Cladding fatigue
5) Cladding collapse
6) Fuel rod stresses

ACRONYMS AND ABBREVIATIONS

Term	Definition
ANS	American Nuclear Society
ANSI	American National Standards Institute
AOO	Anticipated Operational Occurrences
BOC	Beginning of Cycle
BOL	Beginning of Life (bundle)
BWR	Boiling Water Reactor
EOC	End of Cycle
EOL	End of Life (bundle)
GNF	Global Nuclear Fuel
GSTRM	GESTR – Mechanical Fuel Rod Model
HPCI	High Pressure Coolant Injection
HPCS	High Pressure Core Spray
LFWH	Loss of Feed Water Heating
LWR	Light Water Reactor
MOC	Middle of Cycle
MOP	Mechanical Overpower
PCI	Pellet/Cladding Interaction (failure)
TOP	Thermal Overpower
PCMI	Pellet/Cladding Mechanical Interaction
PWR	Pressurized Water Reactor
RCIC	Reactor Core Isolation Cooling
RWE	Rod Withdrawal Error
SCC	Stress Corrosion Cracking
TIG	Tungsten Inert Gas
USNRC	United States Nuclear Regulatory Commission

1. INTRODUCTION

A primary consideration in the design and operation of nuclear power plants is the limitation of radioactive species release from the power plant site. Radioactive species are generated within the fuel rod uranium (and uranium-gadolinium) dioxide pellets as a normal product of the nuclear fission process. Therefore, the fuel rod cladding surrounding the uranium dioxide fuel pellets represents an important barrier to the release of radioactive fission products to the reactor coolant. Although the nuclear power plant system is designed to accommodate a level of activity release that may result from defective fuel rods, while conforming to authorized site activity release limits, the GNF fuel rod design objective is to preclude systematic defects arising under the conditions of authorized operation including normal steady-state operation and anticipated operational occurrences.

This fuel rod design objective is achieved by the imposition of mechanistic limits on the predicted performance of the fuel under the conditions of authorized operation. The GNF GESTR-Mechanical (GSTRM) fuel rod thermal-mechanical performance model (Reference 1) is applied to provide conservative fuel performance predictions for comparison against the specified performance limits. These design and licensing basis analyses are described in detail in this report. The results of these analyses demonstrate that all specified limits are met by the GE14 fuel design.

The fuel rod design analysis methodology is comprised of three elements:

1. Design criteria - Mechanistic design criteria are applied to those fuel rod parameters that realistically represent fuel rod integrity limitations,

2. The analytical GSTRM model (Reference 1) - This fuel rod model calculates the thermal-mechanical changes within the fuel rod which occur during reactor operation and provides a realistic assessment of the response of each design parameter. GSTRM has been developed and qualified based on an extensive experimental fuel rod data base which enables clear quantification of the model prediction uncertainty, and

3. Statistical and worst tolerance analysis procedures – The statistical analysis methodology, in conjunction with the GSTRM model, enables a realistic assessment of statistical uncertainties of the characteristic fuel rod behavior parameters, e.g. fuel rod pressure and pellet temperature as a function of the statistical model parameter input distribution, e.g. pellet diameter and pellet density. The statistical analysis methodology enables direct quantitative assessment of the conservatism of the analysis results. The worst tolerance analysis methodology, in conjunction with the GSTRM model, enables a bounding assessment of the cladding circumferential strain during an anticipated operational occurrence. In this case, the GSTRM inputs important to this analysis are all biased to the fabrication tolerance extreme in the direction that produces the most severe result.

The design criteria and analysis procedures are described in Sections 3 and 4. The results of application to the GE14 fuel design are summarized in Section 5. These results demonstrate

that all criteria are met by the GE14 fuel design up to a peak pellet exposure of [[ ]], corresponding to a fuel rod average exposure of approximately [[ ]] for the UO_2 rods.

2. FUEL ROD DESCRIPTION

The basic GE14 fuel rod is comprised of a column of right circular cylinder fuel pellets enclosed by a cladding tube and sealed gas-tight by plugs inserted in each end of the cladding tube. The plugs are TIG or resistance welded after insertion. The fuel pellets consist of sintered uranium-dioxide (UO_2) or UO_2-gadolinia solid solution ($(U, Gd)O_2$) with a ground cylindrical surface, flat ends, and chamfered edges. Each full-length UO_2 fuel rod may include natural enrichment UO_2 pellets at each end of the fuel pellet column. The fuel rod cladding tube is comprised of Zircaloy-2 with a metallurgically bonded inner zirconium layer.

Each fuel rod includes a plenum at the top of the fuel rod to accommodate the release of gaseous fission products from the fuel pellets. This gas plenum includes a compression spring to minimize fuel column movement during fuel assembly shipping and handling operations while permitting fuel column axial expansion during operation. The GE14 fuel assembly contains 14 fuel rods, which are reduced in length relative to the remaining fuel rods. All fuel rods are internally pressurized with helium to [[ ]] bar to reduce the compressive hoop (and radial) stress induced in the cladding tube by the coolant pressure and to improve the fuel-to-cladding heat transfer.

Figure 2 –1 shows a sketch of the GE14 fuel rods while Figure 2-2 shows a sketch of the GE14 fuel pellet. The characteristic data of the pellet, fuel rod and the cladding are listed in Table 2-1, Table 2-2 and Table 2-3. Materials properties of the pellets and the cladding can be found in Reference 5. Additional details concerning cladding fabrication processing are included in Appendix B.

Table 2-1 Fuel Pellet Characteristics[1]

Item	Value
Material	UO_2, $(U, Gd)O_2$
Melting Temperature[2] UO_2[3] $(U, Gd)O_2$	[[
Enrichment	
Gadolinia Concentration	
Density UO_2 $(U, Gd)O_2$	
Densification[4]	
Fuel Pellet Outside Diameter	
Fuel Pellet Height	
Surface Roughness	]]

[1] Valid at 20 °C
[2] Values shown are valid at beginning-of-life. The melting temperature decreases with exposure at the rate of [[ ]]
[3] The value shown is a conservative estimate of the UO_2 melting temperature.
[4] In-reactor fuel densification is exposure dependent. The value shown represents the fabrication maximum based on a 1700 °C 24-hour resinter test.

Table 2-2 Fuel Rod Characteristics[5]

Item	Value
Fuel Rod Length (shoulder to shoulder)	[[
Full-Length Rod (Basic + Gadolinia)	
Part-Length Rod	
Active Fuel Length	
Full-Length Rod (Basic)	
Full-Length Rod (Gadolinia)	
Part-Length Rod	
Plenum Length/Volume	
Full-Length Rod (Basic)	
Full-Length Rod (Gadolinia)	
Part-Length Rod	
Fill Gas Pressure	
Fill Gas Composition	]]

[5] Valid at 20 °C

Table 2-3 Cladding Tube Characteristics[6]

Item	Value
Material	Zircaloy-2, [[ ]] with zirconium liner
Density	[[
Outside diameter	
Inside diameter	
Cladding Thickness	
Zirconium liner thickness	
Minimum yield strength	
Minimum ultimate tensile strength	
Young's modulus	
Poisson's ratio	
Thermal conductivity	
Surface roughness	]]

[6] Valid at 20 °C

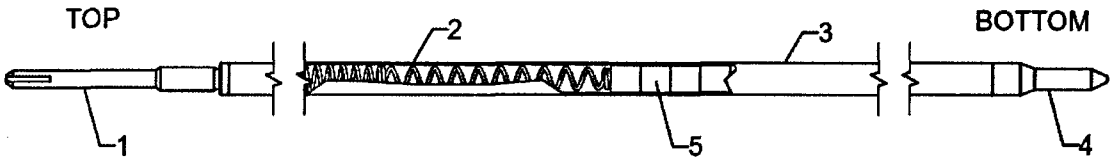

ITEM	TITLE	MATERIAL
1	PLUG, UPPER	ZIRCALOY
2	PLENUM SPRING	STAINLESS STEEL
3	TUBE	ZIRCALOY-2 WITH ZIRCONIUM LINER (BARRIER)
4	PLUG, LOWER	ZIRCALOY
5	PELLET	UO_2 ENRICHED

Figure 2-1 Fuel Rod

[[

]]

Figure 2-2 Fuel Pellet Sketch

3. DESIGN CRITERIA

A set of design limits are defined, and applied in the fuel rod thermal-mechanical design analyses, to ensure that fuel rod mechanical integrity is maintained throughout the fuel rod design lifetime. The design criteria were developed by GNF and other specific industry groups to focus on the parameters most significant to fuel performance and operating occurrences that can realistically limit fuel performance. The specific criteria are patterned after ANSI/ANS-57.5-1981 (Reference 2) and NUREG-0800 Rev. 2 (Reference 3). Table 3-1 presents a summary of the design criteria. The bases for the design criteria listed in Table 3-1 are presented below.

3.1 Cladding Lift-Off / Fuel Rod Internal Pressure (Item 1 of Table 3-1)

The fuel rod is filled with helium during manufacture to a specified fill gas pressure. With the initial rise to power, this fuel rod internal pressure increases due to the corresponding increase in the gas average temperature and the reduction in the fuel rod void volume due to fuel pellet expansion and inward cladding elastic deflection due to the higher reactor coolant pressure. With continued irradiation, the fuel rod internal pressure will progressively increase further due to the release of gaseous fission products from the fuel pellets to the fuel rod void volume. With further irradiation, a potential adverse thermal feedback condition may arise due to excessive fuel rod internal pressure.

In this case, the tensile cladding stress resulting from a fuel rod internal pressure greater than the coolant pressure causes the cladding to deform outward (cladding creep-out). If the rate of the cladding outward deformation (cladding creep-out rate) exceeds the rate at which the fuel pellet expands due to irradiation swelling (fuel swelling rate), the pellet-cladding gap will begin to open (or increase if already open). An increase in the pellet-cladding gap will reduce the pellet-cladding thermal conductance thereby increasing fuel temperatures. The increased fuel temperatures will result in further fuel pellet fission gas release, greater fuel rod internal pressure, and correspondingly a faster rate of cladding creep-out and gap opening.

This potential adverse thermal feedback condition is avoided by limiting the cladding creep-out rate, due to fuel rod internal pressure, to less than or equal to the fuel pellet irradiation swelling rate. This is confirmed through the calculation of a design ratio (of internal pressure to critical pressure) as described in Sections 4.2 and 5.1 and ensuring that the calculated design ratio is less than 1.00 at any point in time for all fuel rod types.

3.2 Fuel Temperature (Melting, Item 2 of Table 3-1)

Numerous irradiation experiments have demonstrated that extended operation with significant fuel pellet central melting does not result in damage to the fuel rod cladding. However, the fuel rod performance is evaluated to ensure that fuel rod failure due to fuel melting will not occur. To achieve this objective, the fuel rod is evaluated to ensure that fuel melting during

normal steady-state operation and whole core anticipated operational occurrences is not expected to occur. For local anticipated operational occurrences,[[

]] This fuel temperature limit is specified to ensure that sudden shifting of molten fuel in the interior of fuel rods, and subsequent potential cladding damage, can be positively precluded.

3.3 Cladding Strain

After the initial rise to power and the establishment of steady-state operating conditions, the pellet-cladding gap will eventually close due to the combined effects of cladding creep-down, fuel pellet irradiation swelling, and fuel pellet fragment outward relocation. Once hard pellet-cladding contact (PCMI) has occurred, cladding outward diametral deformation can occur. The consequences of this cladding deformation are dependent on the deformation rate (strain rate).

3.3.1 High Strain Rate (Anticipated Operational Occurrences, Item 3 of Table 3-1)

Depending on the extent of irradiation exposure, the magnitude of the power increase, and the final peak power level, the cladding can be strained due to the fuel pellet thermal expansion occurring during rapid power ramps. This high strain rate deformation can be a combination of (a) plastic deformation during the power increase due to the cladding stress exceeding the cladding material yield strength, and (b) creep deformation during the elevated power hold time due to creep-assisted relaxation of the high cladding stresses. This cladding permanent (plastic plus creep) deformation during anticipated operational occurrences is limited to a maximum of [[ ]].

In non-barrier cladding, fast power ramps can also cause a chemical/mechanical pellet cladding interaction commonly known as PCI/SCC. To prevent PCI/SCC failures in non-barrier cladding, reactor operational restrictions must be imposed. To eliminate PCI/SCC failures without imposing reactor operational restrictions, GNF invented and developed barrier cladding. Barrier cladding utilizes a thin zirconium layer on the inner surface of Zircaloy tubes. The minimum thickness of the zirconium layer is specified to ensure that small cracks which are known to initiate on the inner surface of barrier cladding (the surface layer subject to hardening by absorption of fission products during irradiation) will not propagate through the zirconium barrier into the Zircaloy tube. The barrier concept has been demonstrated by experimental irradiation testing and extensive commercial reactor operation to be an effective preventive measure for PCI/SCC failure without imposing reactor operating restrictions.

3.3.2 Low Strain Rate (Steady-State Operation, no limit in Table 3-1)

During normal steady-state operation, once the cladding has come into hard contact with the fuel, subsequent fuel pellet irradiation swelling causes the cladding to deform gradually outward. The fuel pellet swelling rate is very slow. The effect of this slow fuel pellet expansion is the relaxation of low stresses imposed by the fuel swelling, resulting in a low strain-rate outward creep deformation of the cladding. Similarly, when the fuel rod internal

pressure exceeds the external pressure exerted by the reactor coolant, the cladding will also slowly creep outward. Under both of these conditions, irradiated Zircaloy exhibits substantial creep ductility. For example, Reference 4 reports circumferential tensile creep strains as high as 18% without fracture. For comparison, the imposition of fuel pellet irradiation swelling stresses beginning at the start of irradiation and continuing throughout lifetime to 100 MWd/kgU will result in a low-stress tensile circumferential creep strain of less than [[ ]]. Therefore, no specific limit is applied to low-strain rate cladding deformation.

3.4 Dynamic Loads / Cladding Fatigue (Item 4 of Table 3-1)

As a result of normal operational variations, cyclic loadings are applied to the fuel rod cladding by the fuel pellet. Therefore, the fuel rod is evaluated to ensure that the cumulative duty from cladding strains due to these cyclic loadings will not exceed the cladding fatigue capability. The Zircaloy fatigue curve employed represents a statistical lower bound to the existing fatigue experimental measurements. The design limit for fatigue cycling, to assure that the design basis is met, is that the value of calculated fatigue usage must be less than the material fatigue capability (fatigue usage ≤ 1.00).

3.5 Elastic Buckling / Cladding Creep Collapse (Item 5 of Table 3-1)

The condition of an external coolant pressure greater than the fuel rod internal pressure provides the potential for elastic buckling or possibly even plastic deformation if the stresses exceed the material yield strength. Fuel rod failure due to elastic buckling or plastic collapse has never been observed in commercial nuclear reactors. However, a more limiting condition that has been observed in commercial nuclear reactors is cladding creep collapse. This condition occurs at cladding stress levels far below that required for elastic buckling or plastic deformation. In the early 1970s, excessive in-reactor fuel pellet densification resulted in the production of large fuel column axial gaps in some PWR fuel rods. The high PWR coolant pressure in conjunction with thin cladding tubes and low helium fill gas pressure resulted in excessive fuel rod cladding creep and subsequent cladding collapse over fuel column axial gaps. Such collapse occurs due to a slow increase of cladding initial ovality due to creep resulting from the combined effect of reactor coolant pressure, temperature and fast neutron flux on the cladding over the axial gap. Since the cladding is unsupported by fuel pellets in the axial gap region, the ovality can become large enough to result in elastic instability and cladding collapse.

It is noted in this PWR experience that, although complete cladding collapse was observed in some cases, cladding fracture did not occur in any case, therefore fuel rod failure by this mechanism is not expected. However, the GNF design basis includes ensuring that fuel rod failure will not occur due to cladding collapse into a fuel column axial gap. The origin of the creep collapse analysis procedure applied by GNF to the GE14 fuel design is the USAEC staff technical report on densification of light water reactor fuels issued in 1972 (Reference 6). In response, GNF produced a number of documents that included the creep collapse analysis procedure detailed in Reference 7. The analysis is performed to confirm that creep collapse of free standing cladding (cladding unsupported by fuel pellets) will not occur. The basic

procedure detailed in Reference 7 has been applied by GNF to the GE14 fuel design to demonstrate that creep collapse of the cladding will not occur. The procedure includes deliberately conservative assumptions; including the assumption that fuel densification can result in large axial gaps in the fuel column. GNF has recognized since its introduction that the procedure is very conservative. This is particularly the case for modern GNF fuel designs with current fabrication processes and controls on fuel pellet density and densification.

3.6 Fuel Rod Stresses (Item 6 of Table 3-1)

The fuel rod is evaluated to ensure that fuel rod failure will not occur due to stresses or strains exceeding the fuel rod mechanical capability. In addition to the loads imposed by the difference between the external coolant pressure and the fuel rod internal gas pressure, a number of other stresses or strains can occur in the cladding tube. These stresses or strains are combined through application of the distortion energy theory to determine an effective stress or strain. The applied limit is patterned after ANSI/ANS-57.5-1981 (Reference 2). The figure of merit employed is termed the Design Ratio where

$$Design\ Ratio = \frac{Effective\ Stress}{Stress\ Limit} or \frac{Effective\ Strain}{Strain\ Limit}$$

where the stress or strain limit is the yield stress or strain. The value of the Design Ratio must be less than 1.00.

3.7 Fuel Rod Hydrogen (Item 7 of Table 3-1)

GNF experience has demonstrated that excessive fuel rod internal hydrogen content due to hydrogenous impurities can result in fuel rod failure due to localized hydriding. The potential for primary hydriding fuel rod failure is limited by the application of specification limits on the fuel pellets (less than [[ ]] evolved hydrogen above 1800 °C) in conjunction with fabrication practices that eliminate hydrogenous contaminants from all sources during the manufacturing process.

Table 3-1 Fuel Rod Thermal-Mechanical Design Criteria

Criterion	Governing Equation
1. The cladding creepout rate ($\dot{\varepsilon}_{\text{cladding creepout}}$), due to fuel rod internal pressure, shall not exceed the fuel pellet irradiation swelling rate ($\dot{\varepsilon}_{\text{fuel swelling}}$). Satisfied if design ratio (of internal pressure to critical pressure) is less than 1.00 (Sections 4.2 and 5.1).	$\dot{\varepsilon}_{cladding\,creepout} \leq \dot{\varepsilon}_{fuel\,swelling}$
2. The maximum fuel center temperature (T_{center}) shall remain below the fuel melting point (T_{melt}).	$T_{center} < T_{melt}$
3. The cladding circumferential plastic strain (ε_θ^P) during an anticipated operational occurrence shall not exceed [[ ]].	[[ ]]
4. The fuel rod cladding fatigue life usage ($\sum_i \frac{n_i}{n_f}$ where n_i=number of applied strain cycles at amplitude ε_i and n_f=number of cycles to failure at amplitude ε_i) shall not exceed the material fatigue capability.	$\sum_i \frac{n_i}{n_f} \leq 1.0$
5. Cladding structural instability, as evidenced by rapid ovality changes, shall not occur.	No creep collapse
6. Cladding stresses(σ_g)/strains(ε_g^P) shall not exceed the material yield strength(σ_{ult})/strain(ε_{ult}).	$\sigma_g < \sigma_{ult}$, $\varepsilon_g^P < \varepsilon_{ult}$
7. The as-fabricated fuel pellet evolved hydrogen (C_H is content of hydrogen) at greater than 1800 °C shall not exceed prescribed limits.	[[ ]]

4. DESIGN ANALYSES DESCRIPTION

Most of the fuel rod thermal-mechanical design analyses are performed using the GSTRM fuel rod thermal-mechanical performance model. The GSTRM fuel rod thermal-mechanical model provides best estimate predictions of fuel rod thermal and mechanical performance. The GSTRM analyses are performed for the following conditions:

1. For the fuel rod design analyses under consideration, the input parameters selected for such analyses are based on the most unfavorable manufacturing tolerances ('worst case' analyses) or by using statistical distributions of the input values. Calculations are then performed to provide either a 'worst case' or statistically bounding tolerance limit for the resulting parameters.

2. Operating conditions, in the form of maximum power verses exposure envelopes for each fuel type, are postulated which cover the conditions anticipated during normal steady-state operation and anticipated operational occurrences.

[[

]] An example power-exposure envelope is shown in Figure 4-1. This maximum power versus exposure envelope is then used for all fuel rod thermal-mechanical design analyses to evaluate the fuel rod design features and demonstrate conformance to the design criteria. This maximum steady-state power versus exposure envelope is applied as a design constraint to the reference core loading nuclear design analyses. This maximum steady-state power versus exposure envelope is also applied as an operating constraint to ensure that actual operation is maintained within the fuel rod thermal and mechanical design bases.

With this maximum steady-state power versus exposure envelope, the GSTRM analyses are conservatively performed [[

]] The fuel rod axial power shape is changed three times during each cycle (BOC, MOC, EOC) and simulates the power distribution effects of Burnup Shape Optimization. The relative axial power distributions used for a full length fuel rod are presented in Figure 4-2.

As discussed above, two types of GSTRM analyses are performed, (1) worst tolerance, or (2) probabilistic.

[[

]]

Figure 4-1 Design Basis Power versus Exposure Envelope (Typical)

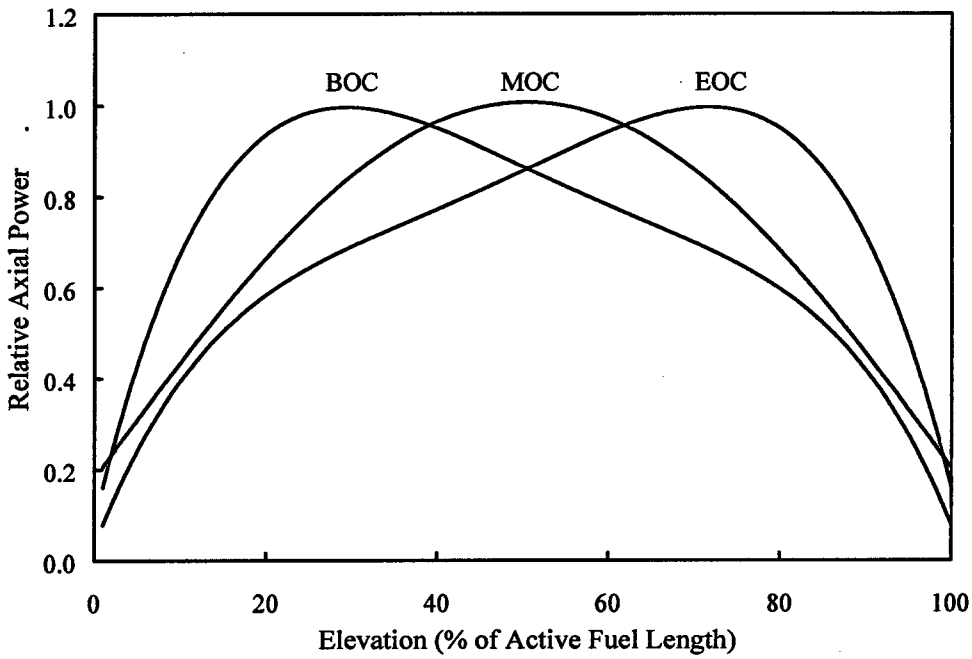

Figure 4-2 Axial Power Distributions (Full Length Fuel Rod)

4.1 Worst Tolerance Analyses

The GSTRM analyses performed to evaluate the cladding circumferential plastic strain during an anticipated operational occurrence applies worst tolerance assumptions. In this case, the GSTRM inputs important to this analysis are all biased to the fabrication tolerance extreme in the direction that produces the most severe result. Table 4-1 presents the analysis fabrication parameter biases and bases for those biases. Other input parameters conservatively biased for this analysis include (a) cladding corrosion (2 sigma), and (b) corrosion product (crud) buildup on the cladding outer surface (2 sigma).

The evaluation reflects continuous operation along the maximum power history according to Figure 4-1, followed by an instantaneous overpower due to an anticipated operational occurrence. The analyses to determine the plastic circumferential strain is performed at several exposure points during the fuel rod lifetime. At the exposure point resulting in the highest circumferential strain the overpower event is increased to determine the maximum permissible overpower that will not exceed the cladding [[ ]] circumferential strain criterion.

The result from this analysis is used to establish the Mechanical Overpower (MOP) discussed in Section 4.5.

Table 4-1 Worst Tolerance Analysis Manufacturing Parameter Biases

Parameter	Bias Direction	Basis

[[

]]

4.2 Statistical Analyses

The remaining GSTRM analyses are performed using standard error propagation statistical methods. The statistical analysis procedure is presented below:

1. The mean value (x_{nom}) and standard deviation (σ_x) of each GSTRM input parameter is determined as discussed in Appendix A. For the manufacturing parameters, these statistical distribution parameter values are determined from the fuel rod drawing tolerances and manufacturing specifications. Certain manufacturing parameters such as pellet density, pellet densification, pellet surface roughness, and cladding surface roughness are controlled by statistical specifications as discussed further in Appendix A. A GSTRM analysis using the limiting power history is performed using the average values of all input parameters. This analysis represents the reference base case analysis and provides the mean values of the output parameters of interest ($y_{reference}$).

2. Then partial derivatives of the resulting parameters as a function of the input parameters are calculated, by first varying independently each input parameter to the ($x_{nom} + 2\sigma_x$) or ($x_{nom} - 2\sigma_x$) value. The direction of the perturbation ($\pm 2\sigma_x$) is taken to increase the severity of the result relative to the performance parameter of interest. These perturbation analyses provide the perturbed values of the output parameters of interest ($y_{perturbation}$). The specific parameters perturbed are specified in Table 4-2.

Table 4-2 GSTRM Parameters Varied Statistically

[[

]]

The nominal values and standard deviations associated with these parameters are derived as discussed in Appendix A. Values are given in Reference 8.

3. The partial derivative of the GSTRM output parameter of interest, with respect to each of the input parameters, is approximately determined as

$$\frac{\partial y}{\partial x} = \frac{y_{perturbation} - y_{reference}}{2\sigma_{x_i}}$$

where

y	=	GSTRM output parameter of interest (e.g., fuel rod internal pressure)
x_i	=	GSTRM input parameter (e.g., cladding thickness)
σ_{x_i}	=	standard deviation of input parameter, x_i

4. The standard deviation of the GSTRM output parameter of interest is then calculated by standard error propagation methods as

$$\sigma_y^2 = \sum_{i=1}^{n}\left[\frac{\partial y}{\partial x_i}\right]^2 \sigma_{x_i}^2 + 2\sum_{i=1}^{n-1}\sum_{j=i+1}^{n}\frac{\partial P}{\partial x_i}\frac{\partial P}{\partial x_j}\sigma_{x_i}\sigma_{x_j}\rho_{x_i x_j}$$

where,

σ_y	Standard deviation of output parameter being analyzed (internal pressure, etc.)
i, j	Index for input variables perturbed in the error propagation analysis
n	Total number of input variables x_i,x_j perturbed in the error propagation analysis
x_i, x_j	Input variable perturbed in the GESTR-Mechanical analysis
$\frac{\partial P}{\partial x_i}, \frac{\partial P}{\partial x_j}$	Partial derivative of output parameter P with respect to perturbed input variable x_i, x_j
$\sigma_{x_i}, \sigma_{x_j}$	Standard deviation of input parameters x_i, x_j
ρ_{x_i,x_j}	Correlation coefficients for variables x_i, x_j

5. [[

]]

The fuel rod internal pressure analysis, the fuel temperature analysis, and the cladding fatigue analysis are all performed statistically in this manner.

4.2.1 Fuel Rod Internal Pressure

For the fuel rod cladding lift-off analysis, the fuel rod internal pressure reflects continuous operation along the maximum steady-state power-exposure envelope throughout lifetime. The standard error propagation analysis results in a mean and standard deviation for the fuel rod internal pressure at various points throughout the design lifetime. At each of these exposure points, the fuel rod internal pressure required to cause the cladding to creep outward at a rate equal to the fuel pellet irradiation swelling rate is also determined using the standard error propagation method. A design ratio is formed based on these two distributions such that, when the design ratio is less than or equal to 1.00, it is assured with at least [[ ]]confidence that the fuel rod cladding will not creep out at a rate greater than the fuel pellet irradiation swelling rate.

4.2.2 Fuel Pellet Temperature

The fuel temperature analysis also reflects continuous operation along the maximum steady-state power-exposure envelope, but is then followed by an instantaneous overpower due to an anticipated operational occurrence. This analysis is performed at several exposure points during the fuel rod lifetime to determine the most limiting time in life. At the most limiting time in life, the magnitude of the overpower event is increased to determine the maximum permissible overpower that will not exceed the incipient fuel center-melting criterion. The result from this analysis establishes the Thermal Overpower (TOP) discussed in Section 4.5.

4.2.3 Cladding Fatigue Analysis

The cladding fatigue analysis also reflects operation along the maximum steady-state power-exposure envelope. However, superimposed on the power-exposure history are power and coolant pressure/temperature changes. The power change spectrum used is listed in Table 4-3.

The fuel duty cycles shown in Table 4-3 represent the conservative assumptions regarding power changes anticipated during normal reactor operation including anticipated operational occurrences, planned surveillance testing, normal control blade maneuvers, shutdowns, and special operating modes such as daily load following. The cladding strain cycles are analyzed using the "rainflow" cycle counting method. The fractional fatigue life expended for each strain cycle is determined and summed over the total number of cycles to determine the total

fatigue life expended over the fuel design lifetime. The material fatigue capability is taken as a lower bound to the available experimental measurements of Zircaloy fatigue capability. The statistical calculation determines the mean and standard deviation of total fatigue life expended. The upper [[ ]] tolerance limit is then determined and required to be < 1.00.

Table 4-3 Fatigue Analysis Power Cycles

Power Cycle, (% Rated)	Frequency, (#/yr.)	Duration
[[		

]]

4.3 Cladding Creep Collapse

This analysis consists of a detailed finite element mechanics analysis of the cladding. The cladding is assumed initially oval shaped. The amount of the initial ovality of the tube may either be assumed to be the allowance for maximum ovality as specified by the design drawings or may be assumed to be the two sigma deviation from roundness based on actual manufacturing data. The specific loading conditions consist of the system coolant pressure applied to the outside of the cladding and the minimum internal as-fabricated pre-pressurization level, as corrected for operating conditions, applied to the inside surface of the cladding. In the GE14 analysis, no support is assumed to be provided from contact of the cladding with the fuel pellets. The creep properties employed are the same as are used in GSTRM. After the condition of maximum ovality is reached at end of life, an overpressure transient is assumed to occur. The magnitude of this overpressure transient is taken to bound the conditions expected during pressurization event anticipated operational occurrences. Application and removal of this overpressure is performed to confirm that collapse due to elastic or plastic instability does not occur.

4.4 Fuel Rod Stress Analysis

The fuel rod stress analysis is performed using the Monte Carlo statistical method. The effects of pressure differential, cladding ovality, radial thermal gradients, spacer contact, thermal bow and circumferential thermal gradients are determined for a specific Monte Carlo trial using classical linear elastic mechanics formulations. For each trial calculation, the stresses are combined into an effective stress using the Von Mises method and compared with the appropriate design limit to produce a design ratio. Design ratios are calculated at the cladding inside and outside diameter, at the spacer and away from the spacer. A large number of trials are performed and the [[ ]] percentile design ratio is determined. Separate analyses are performed to address normal operation and overpower transient conditions, beginning and end-of-life conditions considering both UO_2 and gadolinia fuel rods. In the area of the endplug welds, a finite element mechanics analysis is performed, reflecting the combined effects of the internal-external pressure difference, thermal gradients and axial stresses caused by the differential expansion of the fuel and the cladding.

4.5 Thermal and Mechanical Overpowers

As discussed in Sections 4.1 and 4.2, analyses are performed to determine the values of the maximum overpower magnitudes that would not exceed the cladding circumferential strain criterion (MOP-Mechanical Overpower) and the incipient fuel center-melting criterion (TOP-Thermal Overpower). Conformance to these MOP and TOP criteria is demonstrated as a part of the normal core design and transient analysis process by comparison of the calculated core transient mechanical and thermal overpowers, as defined schematically in Figure 4-3, to the mechanical and thermal overpower limits determined by the GSTRM analyses.

[[

]]

Figure 4-3 Thermal and Mechanical Overpowers (Schematic)

5. DESIGN ANALYSIS RESULTS

5.1 Cladding Lift-Off / Fuel Rod Internal Pressure

The fuel rod internal pressure and (cladding lift-off) design ratio are determined statistically using GSTRM. The analysis is performed for each fuel type to assure with [[ ]] confidence that the fuel rod cladding will not creep outward at a rate greater than the fuel pellet irradiation swelling rate. For the GE14 design, the full length UO_2 rod is limiting relative to internal pressure. Results for the full length UO_2 rod are summarized in Table 5-1.

Table 5-1 Fuel Rod Internal Pressure and Design Ratio

	Value	Exposure MWd/kgU
Maximum Design Ratio	[[	
Nominal EOL Rod Internal Pressure (bar)		]]

In addition to the conservatism inherent in the assumption of operation on a [[ ]] operating envelope, the design ratio in Table 5-1 is based upon conservative assumptions in the calculations of critical pressure (pressure required to result in the cladding creepout rate being equal to the pellet swelling rate), specifically in the assumed pellet swelling rate uncertainty. Even with these conservatisms, the results in Table 5-1 confirm that the GE14 design meets the rod internal pressure criterion.

5.2 Thermal and Mechanical Overpowers

5.2.1 Fuel Temperture

The fuel pellet centerline temperature for the maximum duty fuel rod is statistically determined using GSTRM. Evaluations are performed for each fuel rod type over a range of exposures and overpowers to simulate various AOOs. The evaluations reflect operation on the bounding power-exposure operating envelope prior to the AOO. Based upon the results of these evaluations, the thermal overpower limits in Table 5-2 are applied to the GE14 fuel design to prevent centerline melting.

5.2.2 Cladding Strain

The fuel rod cladding circumferential plastic strain is a 'worst case' analysis (see Section 2.5.1). The parameters, which according to their consequences on the result, that were set at

the extremes in the manufacturing tolerance band are: [[

]].

Evaluations are performed for each fuel rod type over a range of exposures and overpowers to simulate various AOOs. The evaluations reflect continuous operation on the bounding power-exposure operating envelope prior to the AOO. Based upon the results of these evaluations, the mechanical overpower limits in Table 5-2 are applied to the GE14 fuel design to prevent cladding permanent (plastic plus creep) strain equal to or greater than [[ ]].

Table 5-2 LFWH, Inadvertent HPCS, HPCI, RCIC Injection, RWE-Outside Error Cell Overpower Limits

	Maximum Allowable Surface Heat Flux Increase, %	
Event	Thermal (TOP)	Mechanical (MOP)
Core-Wide Transients	[[	
RWE-Outside Error Cell		]]

The thermal overpower (TOP) and mechanical overpower (MOP) limits in Table 5-2 are determined by the limiting [[ ]] rod at its limiting exposure. For rods at non-limiting conditions, separate limits for UO_2 and each UO_2-Gd_2O_3 rod may be applied.

5.3 Cladding Corrosion

The effects of cladding oxidation and corrosion product buildup (crud) on the fuel rod surface are included in the fuel rod thermal-mechanical design evaluations (see Section 2.2.4). The growth rate of the crud and the oxide thickness are input parameters for the statistical analyses. The mean value and standard deviation for the corrosion rate is provided in Appendix A. The input parameters for cladding corrosion are derived from data collected from plants with a range of saturation temperatures and from fuel operating over a wide range of powers. Thus these values and the statistical methodology explicitly address small changes in saturation temperature due to small changes in coolant pressure, such as might occur due to a power uprate.

5.4 Cladding Hydrogen Content

This evaluation relative to hydriding of the fuel rod cladding is based on the substantial operating and manufacturing experience to date with fuel designs fabricated to the same specification limit on the amount of hydrogen permitted in a manufactured fuel rod. This operating experience is summarized in Section 6. The experience with fuel manufactured since

1972 demonstrates that hydriding is not an active failure mechanism for current GNF fuel designs.

5.5 Cladding Creep Collapse

The results of the analysis described in Section 4.3 confirm that the GE14 design will not experience cladding creep collapse.

5.6 Fuel Rod Stresses/Strains

Table 5-3 presents the limiting values of the cladding stress design ratio described in Section 4.4 for rated power and for 30% overpower. The maximum design ratios for both 100% and 130% power occur at BOL. The values between spacers represent the upper 95% value of the design ratios from the Monte Carlo analysis. These results confirm conformance to the cladding stress design criterion.

Table 5-3 Results of Cladding Stress Analysis

	Design Ratio	
Period	Rated Power (100%)	Overpower (130%)
BOL	[[	]]

The maximum effective plastic strain in the lower end plug weld zone, determined by the finite element mechanics analysis described in Section 2.3.4, is [[ ]]. This value occurs at BOL. The limit for this strain is [[ ]]. Thus this result confirms conformance to the end plug weld plastic strain design criterion.

5.7 Dynamic Loads / Cladding Fatigue

Table 5-4 shows the results of the cladding fatigue analysis as performed according to Section 4.2.3. The [[ ]] tolerance limit of the calculated distribution is listed for the full length UO_2 rod and the limiting gadolinia rod. These results confirm conformance to the cladding fatigue design criterion.

Table 5-4 Cladding-Fatigue Usage

		Fatigue Usage	
Rodtype	Nominal	Upper [[ ]]-Tolerance Limit	Limit for upper [[ ]]-Tolerance Limit
UO_2	[[		
Gad			]]

6. FUEL OPERATING EXPERIENCE UPDATE

A summary of GNF fuel experience with recent designs is presented below. The fuel experience summary addresses GE11/13 (9x9) and GE12/14 (10x10) designs, as summarized below in

Table 6-1 and Table 6-2.

Table 6-1 GE11/13 (9X9) Experience Summary as of 10/31/05

Item	GE11 9x9	GE13 9x9	TOTAL 9x9
Fuel Operated			
Reloads	68	31	99
Bundles	12,460	6,676	19,136
Fuel Rods	922,040	494,024	1,259,184
Lead Exposure, MWd/kgU			
Batch average	53	50	
Peak bundle average	64.8	52	

Table 6-2 GE12/14 (10X10) Experience Summary as of 10/31/05

Item	GE12 10x10	GE14 10x10	TOTAL 10x10
Fuel Operated			
Reloads	27	78	105
Bundles	3,830	15,069	18,899
Fuel Rods	352,360	1,386,348	1,738,708
Lead Exposure, MWd/kgU			
Batch average	50	49	
Peak bundle average	68	67	

REFERENCES

1. "Fuel Rod Thermal-Mechanical Analysis Methodology (GESTR-Mechanical)", NEDC-32079P, August 1992

2. American National Standard for Light Water Reactors Fuel Assembly Mechanical Design and Evaluation, American Nuclear Society Standards Committee Working Group ANS 57.5, ANSI/ANS-57.5-1981.

3. US Nuclear Regulatory Commission Standard Review Plan 4.2 – Fuel System Design, (USNRC SRP 4.2), NUREG-0800 Rev. 2, July 1981.

4. E. F. Ibrahim, Creep Ductility of Cold-Worked Zr-2.5 w/o Nb and Zircaloy-2 Tubes In-Reactor, Journal of Nuclear Materials, Vol. 96 (1981), pgs. 297-304.

5. Y1002C001-600, BWR Fuel and Control Materials Properties Handbook.

6. "USAEC Technical Report on Densification of Light Water Reactor Fuels", November 14, 1972.

7. "Creep Collapse Analysis of BWR Fuel Using CLAPS Model", NEDE-20606-P-A, August 1976.

8. "GE14, UO2 and Gad Rod, Design and Licensing Analysis", DRF J11-03057 Study 199, September1999

Appendix A Statistical Distribution Parameters

The GSTRM statistical fuel rod thermal-mechanical performance analyses require the definition of a mean value and standard deviation for each input parameter. These input parameters can be separated into three categories:

Manufacturing parameters

Model prediction uncertainty

External parameters

The derivation of the input variable statistical distribution parameters is described below for each of these categories.

A.1 Manufacturing Parameters

The statistical analysis input values for the fuel rod manufacturing parameters are determined from the applicable engineering drawings and fabrication specifications. The manufacturing parameter limits may be specified as either in the form of (a) classical design nominal ± a tolerance or as minimum/maximum parameter values, or (b) statistical specifications.

For the case of the classical design nominal ± a tolerance or minimum/maximum specifications, the best estimate (mean) value is taken as the mid-point between the upper and lower tolerance values. The standard deviation of the parameter distribution is determined by assuming that the *total* range represented by the manufacturing tolerances corresponds to two standard deviations on both sides of the best estimate value.

Certain manufacturing parameters are controlled by the application of statistical specifications. In this case, the distribution parameters are specified and controlled explicitly. Limit values are specified for both the upper and lower 95% confidence interval on the distribution mean. Limit values are also specified for the upper and lower 95/95 distribution limits. [[

]]

[[

]]

Figure A-1 UO_2 Pellet Density Statistical Specification and Sampling Results

A.2 Model Prediction Uncertainty

The GSTRM fuel rod thermal-mechanical performance model has been developed as a best estimate predictor of fuel performance. Verification of the best estimate prediction capability is provided by the extensive experimental qualification documented in Reference 1. Therefore, the best estimate value of a given output parameter, such as fuel center temperature, is provided by GSTRM when all input parameters are set at their best estimate values.

The GSTRM model prediction uncertainty has been derived through recognition that the fuel rod is a highly thermally driven system. Figure A-2 has been extracted from Reference 1 and presents the comparison of GSTRM fuel temperature predictions to experimentally determined temperatures obtained by direct in-reactor measurement by fuel central thermocouples. As

indicated by Figure A-2, the magnitude of the uncertainty in predicted fuel temperatures increases in proportion to the magnitude of the temperature, indicating a constant percentage uncertainty. Since the fuel pellet temperature drop is directly proportional to the fuel rod power level, a constant percentage uncertainty in fuel temperature is equivalent to a constant percentage uncertainty in effective power level. [[

]]

Again, recognizing that the fuel rod is a highly thermally driven system, [[

]]

[[

]]

Figure A-2 GSTRM Fuel Temperature Experimental Qualification

Figure A-3 presents the GSTRM experimental qualification to the available fission gas release measurements. The variability in Figure A-3 is comprised of (1) the uncertainty in the actual operating power history used for the GSTRM fission gas release prediction, (2) the uncertainty

in the fuel and cladding fabrication parameters as compared to the nominal values used in the GSTRM fission gas release prediction, (3) the uncertainty in the fuel rod puncture/gas collection measurement of the released fission gas inventory, (4) the uncertainty in the accumulated fuel exposure used to define the total generated fission gas inventory, and (5) the true inherent fission gas release model prediction uncertainty. The degree of conservatism introduced by the applied model prediction uncertainty alone [[ ]] is demonstrated in Figure A-4. Figure A-4 presents a comparison of the fission gas release measurements to the GSTRM predictions for the case of a $+2\sigma$ model uncertainty perturbation. Figure A-4 demonstrates that the model uncertainty perturbation alone results in an overprediction of [[ ]] of the fission gas release measurements.

A.3 External Parameters

The external parameter inputs to GSTRM include the reactor coolant pressure, the cladding corrosion rate, and the corrosion product (crud) buildup rate. The reactor coolant pressure mean and standard deviation are derived from the operational tolerances specified for this parameter at the full rated power condition. The mean value is taken as equal to the nominal specified coolant pressure. The coolant pressure standard deviation is derived from the coolant pressure operational tolerances by assuming that the total range corresponds to two standard deviations on both sides of the best estimate value.

The cladding corrosion rate and corrosion product (crud) buildup rate statistical distribution values are derived from characterization measurements taken on production fuel rods operating in commercial nuclear reactors. For example, Figure A-5 presents a comparison of the design corrosion model to the available GNF corrosion-resistant cladding oxide thickness measurements as determined by eddy current probe lift-off measurements.

[[

]]

Figure A-3 GSTRM Fission Gas Release Experimental Qualification

[[

]]

Figure A-4 Effect of +2 Sigma Bias in Model Prediction Uncertainty on Fission Gas Release Predictions

[[

]]

Figure A-5 Cladding Corrosion Model Statistical Parameters

Appendix B Fuel Rod Processing

GE14 fuel rods are fabricated in accordance with materials and processing specifications current at the time of fabrication. Currently, the fuel rod is specified to include [[ ]] Zircoloy-2 barrier cladding. This alloy has been used by GNF since before the introduction of reload quantities of barrier fuel in the early 1980s. The cladding process current at the date of this report is denoted P8. Details of the P8 process, including specifications for finished tubes, are as follows.

[[

]]

The alloy composition plus allowable oxygen level for the Zircaloy-2 and zirconium portions of the tube shell are defined in the table below. Other requirements are currently specified in GNF material specification 26A5757 Rev. 4.

Table B-1 Tube Shell Alloy Composition and Oxygen Concentration

	Concentration (weight %)	
Element	Zircaloy-2	Zirconium
Tin	[[	
Iron		
Chromium		
Nickel		
Iron + Chromium + Nickel		
Oxygen		]]

The tube shell is reduced to tubing on Pilger tube reducers. [[

]] The tube is then polished, inspected, cut to size, given a final NaOH clean and a final inspection.

The Zircaloy-2 portion of the finished tube must meet the chemistry and texture requirements in the tables below. In addition, the finished tube must meet requirements on strength, surface finish, corrosion resistance and other aspects that may impact in-reactor performance. All requirements are currently specified in GNF material specification 26A5798 Rev. 5.

Table B-2 Finished Tube Chemistry - Zircaloy-2 Portion

Element	Maximum Concentration (ppm)
Oxygen	[[
Hydrogen	
Nitrogen	]]

Table B-3 Finished Tube Crystallographic Texture - Zircaloy-2 Portion

Direction	Texture Factor
Longitudinal	[[
Radial	
Transverse	]]

Note: f_I is the fraction of basal poles in the I-direction

Periodically, GNF revises the processing of the cladding, primarily to obtain optimum PCI resistance and corrosion performance as fuel operating strategies and plant water chemistries evolve. The impact of such changes on fuel rod thermal-mechanical design and licensing analyses are assessed as follows.

The material properties of Zircaloy based LWR fuel cladding used in thermal-mechanical design and licensing analyses include:

1. Elastic properties (elastic modulus and Poison's ratio)
2. Thermal expansion coefficients
3. Plastic properties (yield and ultimate stress and failure strain)
4. Creep properties
5. Fatigue properties
6. Irradiation growth properties
7. Corrosion properties

The elastic properties and thermal expansion coefficients are only weakly dependent upon alloy composition and more dependent upon fabrication process, specifically the reduction process and the resulting texture. Since GNF has maintained essentially unchanged texture specifications on fuel rods, the periodic process changes will have negligible impact on these properties.

Likewise, the plastic and creep properties are only weakly dependent upon alloy composition. However, these properties are strongly dependent upon the fabrication process, specifically the final heat treatment. Since GNF tubes are [[ ]] at the end of the fabrication process, the periodic process changes will have negligible impact on these properties.

Also, the fatigue and irradiation growth properties are only weakly dependent upon alloy composition and strongly dependent upon the fabrication process, specifically the final heat treatment and texture. Since GNF tubes are [[ ]] at the end of the fabrication process and the texture specifications are essentially unchanged, the periodic process changes will have negligible impact on irradiation growth properties.

Finally, the corrosion properties have a strong dependency on fabrication process, and specifically on the in-process heat treatments. GNF has recognized this dependency and maintains an on-going program to measure and characterize corrosion (and crud) performance for a variety of operating conditions and plant water chemistries. These characterizations are used to determine corrosion and crud statistical distributions for thermal-mechanical analyses of GNF fuel rods and are updated when the data indicates an update is necessary. Thus the potential changes in corrosion performance of GNF fuel rods due to both periodic process

changes and changing water chemistries in the plants are directly addressed by the GNF design and licensing process.

In summary, the material properties used in GNF fuel rod design and licensing analyses adequately address periodic minor changes in the cladding fabrication process that may be made for GE14 cladding to optimize PCI resistance and corrosion performance. If more significant process changes are made, the applicability and adequacy of the properties will be confirmed. It will also be confirmed that the impact on in-reactor performance and reliability will be acceptable.